

Research Article
Implant Science



Comparison of microbiome profiles across sample types in patients with peri-implantitis using 16S rRNA sequencing

Da-Mi Kim [†], Inpyo Hong [†], Joo-Yeon Lee , Seulbin Im ,
Kyeong-Won Paeng , Ui-Won Jung , Jae-Kook Cha *

Department of Periodontology, Research Institute for Periodontal Regeneration, Yonsei University College of Dentistry, Seoul, Korea



Received: Apr 2, 2025
Revised: Jul 22, 2025
Accepted: Jul 23, 2025
Published online: Dec 2, 2025

*Correspondence:

Jae-Kook Cha

Department of Periodontology, Research Institute for Periodontal Regeneration, Yonsei University College of Dentistry, 50-1 Yonsei-ro, Seodaemun-gu, Seoul 03722, Korea.
Email: chajaekook@gmail.com
Tel: +82-2-2228-3185

[†]Da-Mi Kim and Inpyo Hong contributed equally to the study.

Copyright © 2026. Korean Academy of Periodontology
This is an Open Access article distributed under the terms of the Creative Commons Attribution Non-Commercial License (<https://creativecommons.org/licenses/by-nc/4.0/>).

ORCID iDs

Da-Mi Kim
<https://orcid.org/0009-0008-1124-7929>
Inpyo Hong
<https://orcid.org/0000-0002-0486-9593>
Joo-Yeon Lee
<https://orcid.org/0000-0002-6424-3605>
Seulbin Im
<https://orcid.org/0009-0001-3741-3007>
Kyeong-Won Paeng
<https://orcid.org/0000-0001-7262-7345>
Ui-Won Jung
<https://orcid.org/0000-0001-6371-4172>
Jae-Kook Cha
<https://orcid.org/0000-0002-6906-7209>

<https://jpis.org>

ABSTRACT

Purpose: Numerous studies have applied microbial analyses to peri-implantitis, including analyses of samples collected from various sites. While characteristics of the peri-implantitis microbiome have been identified, differences in sampling methods between studies have not been considered. The present study aimed to (1) characterize microbial similarities among saliva, gingival crevicular fluid (GCF), subgingival plaque (SGP) and inflammatory connective tissue (ICT) within the same participant with peri-implantitis; and (2) determine the microbial profiles of peri-implantitis sites.

Methods: Saliva, GCF, and SGP samples were collected from 18 patients undergoing peri-implantitis surgery, and ICT samples were obtained after flap elevation. The collected samples were analyzed using 16S rRNA sequencing.

Results: The sampling sites showed a mean bone loss of 6.9 mm and a maximum probing depth (PD) of 8.3 mm. Alpha diversity did not differ significantly among ICT, GCF, and SGP, whereas saliva exhibited a distinct diversity profile. Additionally, beta diversity analyses indicated that the microbial community structure differed significantly between saliva and the other samples. In taxonomic analyses, the microbial profiles of ICT, GCF, and SGP were clearly distinguishable from those of saliva. Saliva had lower proportions of Bacteroidetes and higher proportions of Proteobacteria and Actinobacteria species, especially at sites with deep PD. Pearson correlation analyses revealed strong correlations between ICT and both GCF and SGP, but not between ICT and saliva. Pathogenic species such as *Porphyromonas gingivalis*, *Tannerella forsythia*, *Treponema denticola*, *Campylobacter rectus*, *Filifactor alocis*, and *Porphyromonas endodontalis* were more abundant in ICT than in saliva.

Conclusions: ICT, GCF, and SGP shared similar microbial profiles, whereas saliva exhibited a significantly different profile. ICT, GCF, and SGP had higher abundances of peri-implant pathogenic species, whereas saliva tended to have lower abundances; this difference was especially pronounced in deep pockets.

Keywords: 16S rRNA; Microbiome; Peri-implantitis; RNA sequencing

Funding

This work was supported by a National Research Foundation of Korea (NRF) grant funded by the Korean government (MSIT) (RS-2025-00522998).

This research was also supported by the Bio & Medical Technology Development Program of the National Research Foundation (NRF) funded by the Korean government (MSIT) (No. 2022M3A9F3016364).

The biospecimens and data used in this study were provided by the Biobank of Yonsei University Dental Hospital, a member of the Korea Biobank Network (project No. 2024ER050700).

Conflict of Interest

No potential conflict of interest relevant to this article was reported.

Author Contributions

Conceptualization: Jae-Kook Cha; Formal analysis: Inpyo Hong, Da-Mi Kim; Investigation: Da-Mi Kim, Joo-Yeon Lee, Seulbin Im, Kyung-Won Paeng; Methodology: Inpyo Hong, Jae-Kook Cha; Project administration: Jae-Kook Cha; Writing - original draft: Inpyo Hong, Da-Mi Kim; Writing - review & editing: Jae-Kook Cha, Ui-won Jung.

INTRODUCTION

Peri-implantitis is primarily driven by microbiome dysbiosis that triggers the inflammatory response, leading to degradation of the supporting bone and soft tissues [1,2]. Accordingly, identifying pathogenic microbial changes in peri-implantitis can improve the understanding of disease progression, enabling more accurate diagnoses and more effective treatments. Traditional culture-based methods are inadequate for microbial analyses of peri-implantitis [3]. However, recent advances in 16S rRNA sequencing have revolutionized the understanding of microbial diversity [4,5]. 16S rRNA sequencing analyzes the unique ribosomal RNA of microbial species to provide a comprehensive overview of the microbial communities present at different sampling sites [6,7].

Saliva, gingival crevicular fluid (GCF), and subgingival plaque (SGP) samples can be collected non-invasively and are rich in biomarkers such as microorganisms, proteins, and cytokines. These samples have been widely used to diagnose diseases and analyze the microbiome [4-8]. However, in microbial analyses, the bacteria collected from GCF and saliva represent those washed out from the SGP, whereas those collected from inflammatory connective tissue (ICT) reflect organisms that have invaded through the sulcular epithelium.

ICT has been analyzed to elucidate the pathology of periodontal disease, since the inflammatory response is initiated by bacteria that penetrate the host defenses of the epithelium in the gingival sulcus [9,10]. Because sampling ICT involves directly obtaining inflamed tissue from peri-implantitis sites, it may provide deeper insight into host-pathogen interactions. Pathogenic bacteria such as *Porphyromonas gingivalis* and *Tannerella forsythia* have been identified within ICT at periodontitis lesions [11]. Furthermore, recent studies using single-cell RNA sequencing of keratinocytes from ICT have revealed cell-bacteria interactions and regulation of immune responses through cell communication [9].

Previous studies analyzing various samples using 16S rRNA sequencing have focused on the microbial changes associated with peri-implantitis [4,5,12-15]. To the best of our knowledge, no studies have compared the microbial profiles of different samples collected from the same participant. If microbial profiles vary significantly depending on the sampling method, this should be considered when analyzing peri-implantitis microbiome data.

By comparing microbial similarities across different sampling methods from the same lesion, this study aims to guide the selection of clinically relevant and microbiologically representative sampling strategies for the microbial analysis of peri-implantitis. Therefore, the aims of the present study were (1) to characterize microbial similarities among saliva, GCF, SGP, and ICT within the same participant with peri-implantitis; and (2) to determine the microbial profiles of peri-implantitis sites using 16S rRNA sequencing.

MATERIALS AND METHODS

Patient population

This study enrolled 18 patients receiving peri-implantitis treatment at the Department of Periodontics, Yonsei University Dental Hospital, Seoul, South Korea. These patients had been diagnosed with peri-implantitis (radiographically confirmed peri-implant bone loss ≥ 3 mm and probing depth [PD] ≥ 6 mm, with bleeding and/or suppuration on probing) and

were scheduled for surgical treatment [1]. The exclusion criteria were: (1) history of surgical treatment for peri-implantitis; (2) untreated periodontitis; (3) smoking; (4) pregnancy; (5) use of drugs affecting periodontal tissues; (6) uncontrolled diabetes mellitus or other systemic diseases; (7) need for antibiotic prophylaxis; or (8) history of antibiotic intake in the previous 3 months. Clinical parameters were evaluated with a periodontal probe (CP15, Nordent Manufacturing, Elk Grove Village, IL, USA). Periapical radiographs were obtained for radiographic analyses.

If a patient had multiple implants fulfilling the inclusion criteria, the implant with the deepest PD was included in the study. Written informed consent was obtained from all patients after the study was explained. Ethics approval was granted by the Institutional Review Board for Clinical Research at the Dental Hospital of Yonsei University (approval number: 2-2020-0106). After initial screening, plaque control was performed with a metallic copper-alloy ultrasonic scaler tip (IS TIP; B&L Biotech, Ansan, Korea). All patients received the same type of toothbrush and toothpaste, along with standardized oral hygiene instructions, to use until surgical treatment.

Sample collection

Sample collection followed the standard operating procedures (SOP) for the collection, processing, and storage of oral biospecimens at the Korea Oral Biobank Network [16]. This SOP includes detailed protocols for the collection, management, and storage of oral biospecimens.

All participants were asked to refrain from eating, rinsing with mouthwash, or toothbrushing for at least 3 hours prior to sample collection to avoid contamination. They were also asked to rinse their mouths with water to remove residual debris and then rest for 5–10 minutes to eliminate remaining moisture from the rinse. Unstimulated saliva (5 mL) was collected by passive drooling into a sterile 50-mL conical tube (SPL Life Sciences Co., Ltd., Pocheon, Korea) over 5–10 minutes (**Figure 1A**) [17]. GCF was collected by inserting a sterile paper point (size #20) into the gingival sulcus [8]. The implant area was carefully isolated and dried with a 3-way syringe, and a sterile paper point was gently inserted into the gingival sulcus at the site with the deepest PD for 20 seconds, avoiding contamination from plaque and saliva (**Figure 1B**). SGP samples were collected using sterile titanium curettes [18]. After removing the implant prosthesis and supragingival biofilm, the peri-implantitis site was isolated with a 3-way syringe and a cotton pellet. A titanium curette (IMPLG1/2T, Hu-Friedy, Chicago, IL, USA) was then applied in a single vertical stroke of moderate pressure against the implant surface to collect the SGP (**Figure 1C and D**). All saliva, GCF, and SGP samples were immediately immersed in RNA stabilizing reagent (RNAlater, Thermo Fisher Scientific, Waltham, MA, USA) and stored at -80°C within 10 minutes of collection for subsequent analyses [16].

Following the collection of saliva, GCF, and SGP samples, local anesthesia was administered, and a sulcular incision was made for surgical treatment. A full-thickness flap was gently elevated and rinsed with sterile saline before excising the ICT sample from around the peri-implantitis defects with a sterile titanium curette, following an internal bevel incision (**Figure 1E and F**) [11]. ICT samples were immediately placed in sterile saline tubes and stored at -80°C for subsequent processing. After granulation tissue was collected, surgical peri-implantitis treatment was performed according to the protocol detailed previously [2].

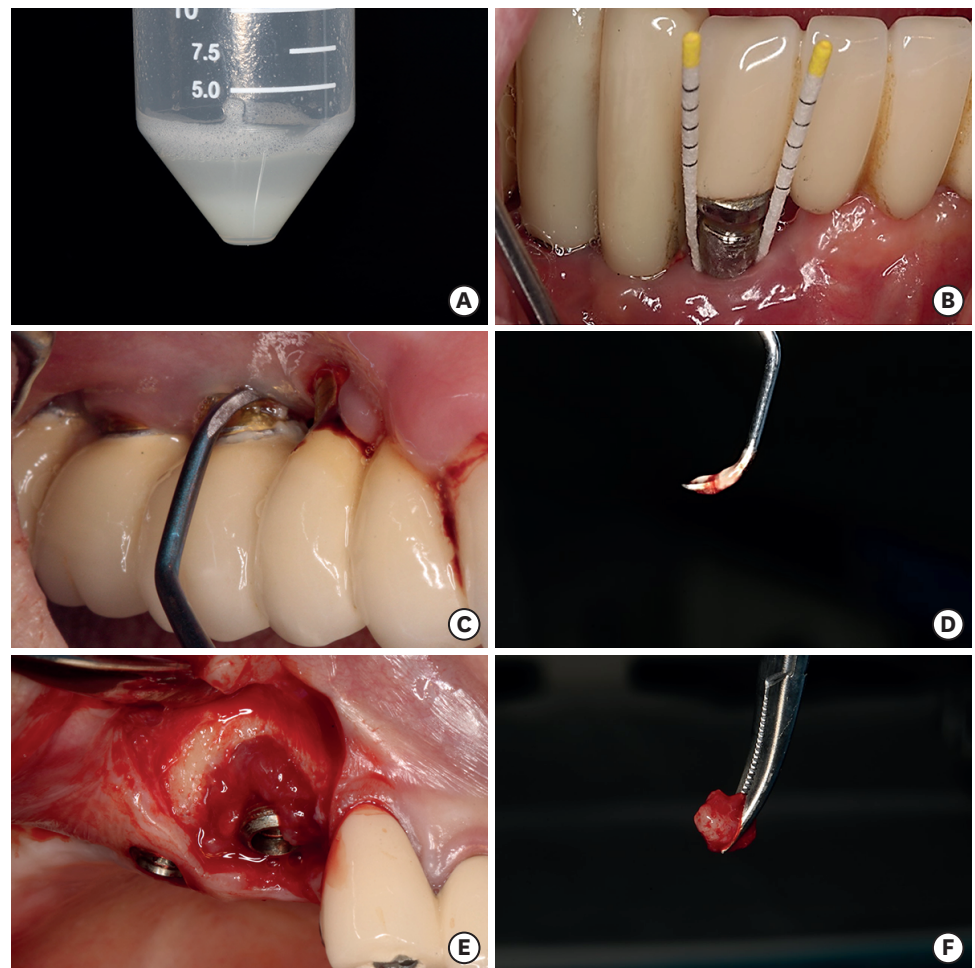


Figure 1. Representative sample collection from a patient with peri-implantitis. (A) Saliva sample. (B) Gingival crevicular fluid sampling. (C) SGP collection. (D) Collected SGP sample. (E) ICT around a peri-implantitis lesion. (F) Collected ICT sample.
SGP: subgingival plaque, ICT: inflammatory connective tissue.

16S rRNA gene sequencing

For GCF and SGP sample preparation, GCF-soaked paper points and SGP were placed in Lysing Matrix E tubes (MP Biomedicals, Irvine, CA, USA), and 978 μ L of sodium phosphate buffer and 122 μ L of Matrix T buffer (MP Biomedicals) were added. Saliva (800 μ L) was transferred to Lysing Matrix E tubes, followed by 200 μ L of sodium phosphate buffer and 122 μ L of Matrix T buffer. For ICT sample preparation, 50 mg of ICT was homogenized using liquid nitrogen and then combined with 978 μ L of sodium phosphate buffer and 122 μ L of Matrix T buffer. All samples were homogenized using liquid nitrogen. After preparation, samples were processed on a FastPrep instrument for 40 seconds at a speed of 6 meters per second to disrupt the cell walls and release nucleic acids. Total bacteria genomic DNA was extracted from all samples using the FastDNA Spin kit (MP Biomedicals). Beads were added, and samples were further disrupted for 40 seconds using a TissueLyser device (Qiagen, Hilden, Germany). PCR amplification was performed with fusion primers targeting the V3–V4 region of the 16S rRNA gene using the extracted DNA: 341F, 5'-AATGATACGGCGACCACCGAGATCTACAC-XXXXXXXXX-TCGTCGGCAGCGTCAGATGTGTATAAGAGACAG-CCTACGGGNGGCWGCAG-3'; and 805R, 5'-CAAGCAGAAGACGGCATACGAGAT-XXXXXXXXXGTCTCGTGGGCTCGG-

AGATGTGTATAAGAGACAG-GACTACHVGGGTATCTAATCC-3'. The fusion primers were constructed in the following order: P5 (P7) graft binding sequence, i5 (i7) index, Nextera consensus, sequencing adapter, and target region sequence. The PCR conditions included initial denaturation at 95°C for 3 minutes, 25 cycles of denaturation at 95°C for 30 seconds, primer annealing at 55°C for 30 seconds, and extension at 72°C for 30 seconds, with a final extension at 72°C for 5 minutes. The V3–V4 hypervariable region of the 16S rRNA gene was sequenced on the MiSeq platform (Illumina, San Diego, CA, USA).

Raw data preparation and statistical analyses

Raw paired-end Illumina sequences were processed using the dada2 pipeline (version 1.32.0) as described previously [19]. In brief, primer sequences were trimmed, and reads were filtered using the filterAndTrim function to remove those with more than 4 (forward) and 6 (reverse) expected errors based on quality scores and truncated at 280 base pairs (forward) and 260 base pairs (reverse). The dada2 algorithm was applied to infer exact amplicon sequence variants (ASVs) from the processed sequences and to remove chimeras. Taxonomy was assigned to the ASVs using a naive Bayesian classifier against the expanded Human Oral Microbiome Database (version 15.1, The Forsyth Institute, Cambridge, MA, USA) with a minimum bootstrap confidence of 50. An ASV table was constructed by recording the number of times each ASV was observed in each sample.

The ASV table, sample data, and taxonomy table were imported into the R environment as phyloseq objects (version 1.48.0) [20]. Additional sample data categories were added to the phyloseq sample data table. ASVs with no phylum assigned were filtered out, and counts were agglomerated at the species level. Alpha and beta diversity metrics were calculated on the filtered ASV table using the estimate_richness and ordinate functions in the phyloseq package. All plots were generated using the ggplot2 package (version 3.5.1). Heat maps were drawn with the ComplexHeatmap package (version 2.20.0) [21]. All statistical analyses and visualizations were performed in R (version 4.4.1; R Foundation for Statistical Computing, Vienna, Austria) and RStudio.

This study was designed as an exploratory, within-subject comparison of microbiome profiles across different sampling methods from peri-implantitis lesions. Therefore, no formal sample size calculation was performed. A total of 18 patients were enrolled, each contributing 4 sample types. This sample size was considered appropriate for non-parametric paired statistical analyses.

For the statistical analyses, samples from the same participant were paired. The microbial community richness and diversity (alpha diversity) of the samples were quantified using the Shannon index. Microbiome characteristics (beta diversity) were compared using principal coordinate analysis. Scatter plots were generated to compare microbial abundance ranks between different samples, with the x- and y-axes representing the ranks of a particular species in ICT and its paired sample from the same participant, respectively. Correlations between the samples were assessed by comparing Spearman correlation coefficients of ICT and the other samples using the Fisher *Z* test. The abundance ranks and relative abundances of 7 known pathogenic bacterial species related to peri-implantitis (*P. gingivalis*, *T. forsythia*, *Treponema denticola*, *Campylobacter rectus*, *Filifactor alocis*, *Fusobacterium nucleatum*, and *Porphyromonas endodontalis*) were pairwise ranked using the Friedman test [5,12,13,22]. Subgroup analyses were applied based on PD: moderate-PD group, PD=6–8 mm; deep-PD group, PD ≥9 mm [23].

RESULTS

Demographic and clinical characteristics of participants

The demographic and clinical characteristics of the participants are summarized in **Table 1**. None of the participants were smoker. As shown in the table, implants affected by peri-implantitis displayed a median bone loss of 6.7 mm. The deepest PD site—from which both GCF and SGP were collected—had a median PD of 7.5 mm.

Similarities in microbial diversity among saliva, GCF, SGP, and ICT

The Shannon indices did not differ significantly among paired GCF, SGP, and ICT samples, but they did differ between paired saliva samples and the other sample types ($P < 0.05$) (**Figure 2A, Supplementary Table 1**). In the deep-PD group, the Shannon indices for saliva differed significantly from those for paired ICT and GCF samples, whereas no significant inter-sample differences were observed in the moderate-PD group. The results of the beta diversity analyses are presented in **Figure 2B**. The community structure of saliva was clearly distinct from those of the other samples in both study groups.

Table 1. Demographic and clinical characteristics of the subjects

Parameters	Peri-implantitis (n=18)
Patient age (yr)	65 (49–79)
Sex	
Male	5
Female	13
HTN	
Yes	5
No	13
DM	
Yes	5
No	13
Smoking	
Yes	0
No	18
Periodontitis diagnosis	
Stage II	2
Stage III	11
Stage IV	5
Radiographic bone loss	6.7 (2.8–10.5)
PD	6 (3–12)
PD (at deep site sampled)	7.5 (6–12)
Implant type	
Tissue level	1
Bone level	17
Implant prosthesis type	
Screw	9
Cement	9
Location of implant	
Maxilla	7
Mandible	11
Location of implant	
Posterior	18
Anterior	0

Values are presented as median (range).

HTN: hypertension, DM: diabetes mellitus, PD: periodontal disease.

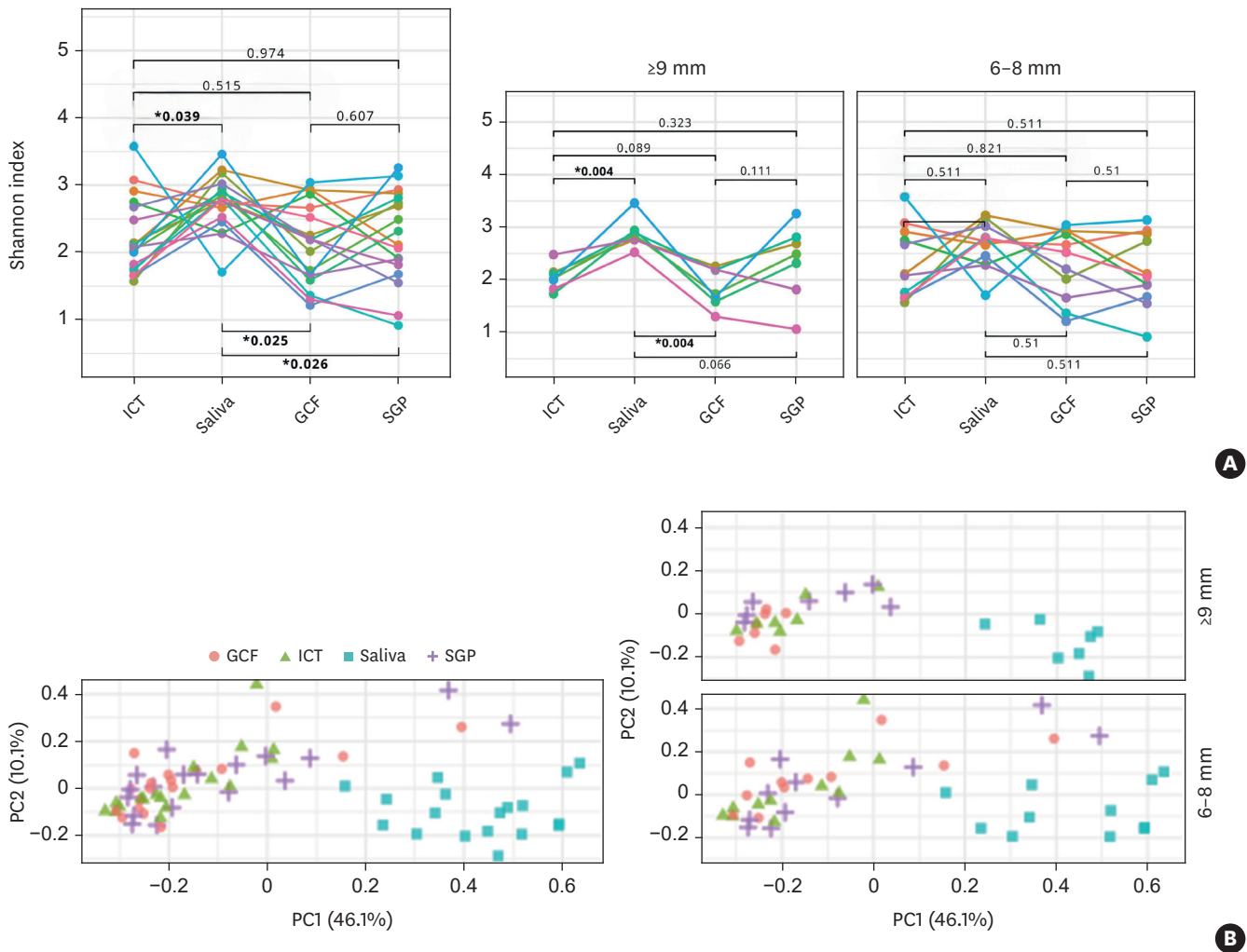


Figure 2. Comparison of microbial diversity among ICT, saliva, GCF, and SGP. (A) Alpha diversity quantified using the Shannon index: saliva differed significantly from the other 3 sample types overall and from ICT and GCF in the deep-probing depth group. (B) Principal coordinate analysis plot comparing beta diversity metrics. Saliva exhibited differences from the other samples in both study groups.

ICT: inflammatory connective tissue, GCF: gingival crevicular fluid, SGP: subgingival plaque, PC: principal component.

* $P < 0.05$.

Taxonomy profiles of peri-implantitis sites and similarity of profiles across collection methods

Overall, saliva exhibited a distinct microbial profile, with a lower proportion of Bacteroidetes and higher proportions of Proteobacteria and Actinobacteria species (Figure 3A). These differences were more pronounced in the deep-PD group (Figure 3B).

Scatter plots comparing the abundance ranks of ICT samples with their paired samples revealed strong positive correlations for ICT versus GCF and ICT versus SGP, with no significant difference between the corresponding Spearman correlation coefficients (Figure 4A, Supplementary Figure 1). In contrast, the correlation for ICT vs. saliva was weak, and the Spearman correlation coefficient for ICT versus saliva was significantly lower than for ICT versus GCF and ICT versus SGP (Figure 4B).



Figure 3. Microbial taxonomic profiles of peri-implantitis ICT, saliva, GCF, and SGP. (A) The overall microbial profile of saliva differed markedly from those of the other samples. (B) Differences between saliva and the other samples were larger in the deep-probing depth group. GCF: gingival crevicular fluid, ICT: inflammatory connective tissue, SGP: subgingival plaque.

Abundance ranks of peri-implantitis pathogenic species

P. gingivalis, *T. forsythia*, *T. denticola*, *C. rectus*, *F. alocis*, and *P. endodontalis* exhibited significantly higher abundance ranks in ICT than in saliva (Figure 5A). In subgroup analyses, this trend was observed in both the deep- and moderate-PD groups (Figure 5B). However, in the deep-PD group, *P. gingivalis* displayed a high abundance rank across all paired samples, with no significant differences between them.

The relative abundances of peri-implantitis pathogenic species are presented in Figure 6. These differed significantly by sample type for the 3 red-complex species (Figure 6A). *P. gingivalis* was markedly lower in saliva, whereas *T. forsythia* and *T. denticola* were significantly more abundant in ICT than in saliva and SGP. Subgroup analyses of the deep- and moderate-PD groups revealed that the relative abundance of *P. gingivalis* was significantly lower in saliva, while *T. forsythia* and *T. denticola* were more abundant in ICT than in saliva in both groups. These differences were particularly pronounced in the deep-PD group (Figure 6B).

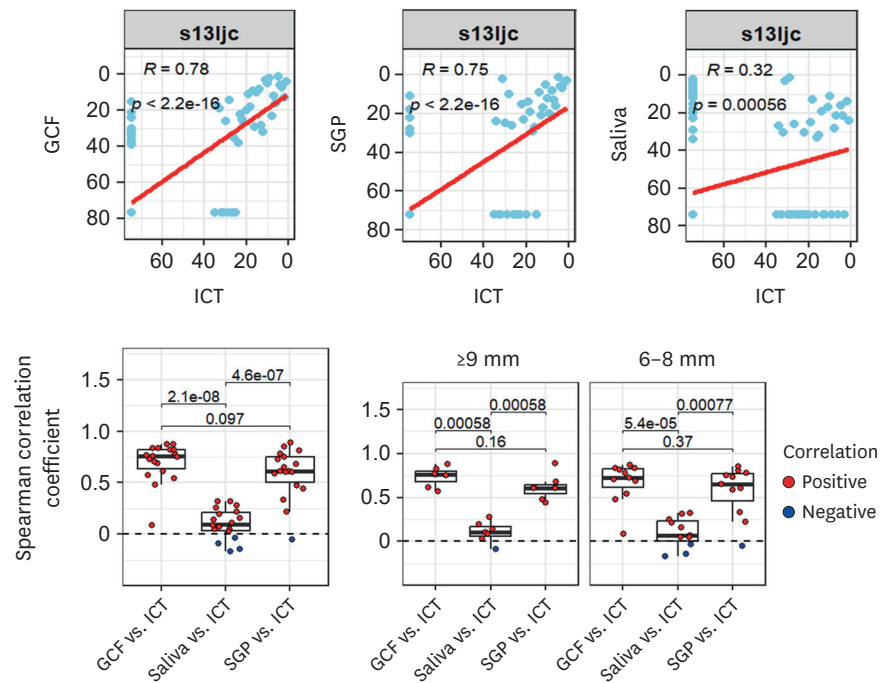


Figure 4. Rank-rank correlations among microbial species abundances. (A) Scatter plots comparing the ranks of microbial species between ICT and other collection sites (GCF, SGP, and saliva) in a single exemplar patient (patient s131jc; scatter plots for all patients are presented in **Supplementary Figure 1**). (B) Box plots of Spearman correlation coefficients for all patients.

ICT: inflammatory connective tissue, GCF: gingival crevicular fluid, SGP: subgingival plaque.

DISCUSSION

This study investigated the microbial profiles of peri-implantitis sites using 16S rRNA sequencing at different sampling sites. The findings revealed similar microbial profiles for ICT, GCF, and SGP, whereas saliva exhibited a significantly different profile, with larger differences at sites with deeper PDs. Analyses of peri-implantitis pathogenic species indicated a similar pattern: ICT, GCF, and SGP displayed higher abundances of these species, while saliva tended to have lower abundances. Notably, at deep-PD sites, *T. forsythia* and *T. denticola* were significantly more abundant in ICT than in saliva.

The oral cavity is a complex ecosystem with various niches used for microbiome analyses [24]. The choice of niche-specific samples varies with the research objectives. For example, Kim et al. [7] analyzed SGP, supragingival plaque, and saliva in patients with periodontitis and found that saliva had the highest diversity and a broader range of species, though with generally lower abundances. Similarly, Zhang et al. [25] reported that saliva from patients with oral cancer displayed higher diversity and significantly different microbial communities compared with dental plaque samples. Consistent with these studies, we found that the microbial communities of saliva differed significantly from those of ICT, GCF, and SGP, with higher diversity and a wider range of low-abundance species. These observations may reflect the role of saliva in transporting microorganisms from multiple oral niches, such as the tongue and buccal mucosa [25]. Therefore, while saliva sampling is convenient, it may underestimate site-specific microbial changes at peri-implantitis sites and display lower abundances of pathogenic species associated with peri-implantitis.

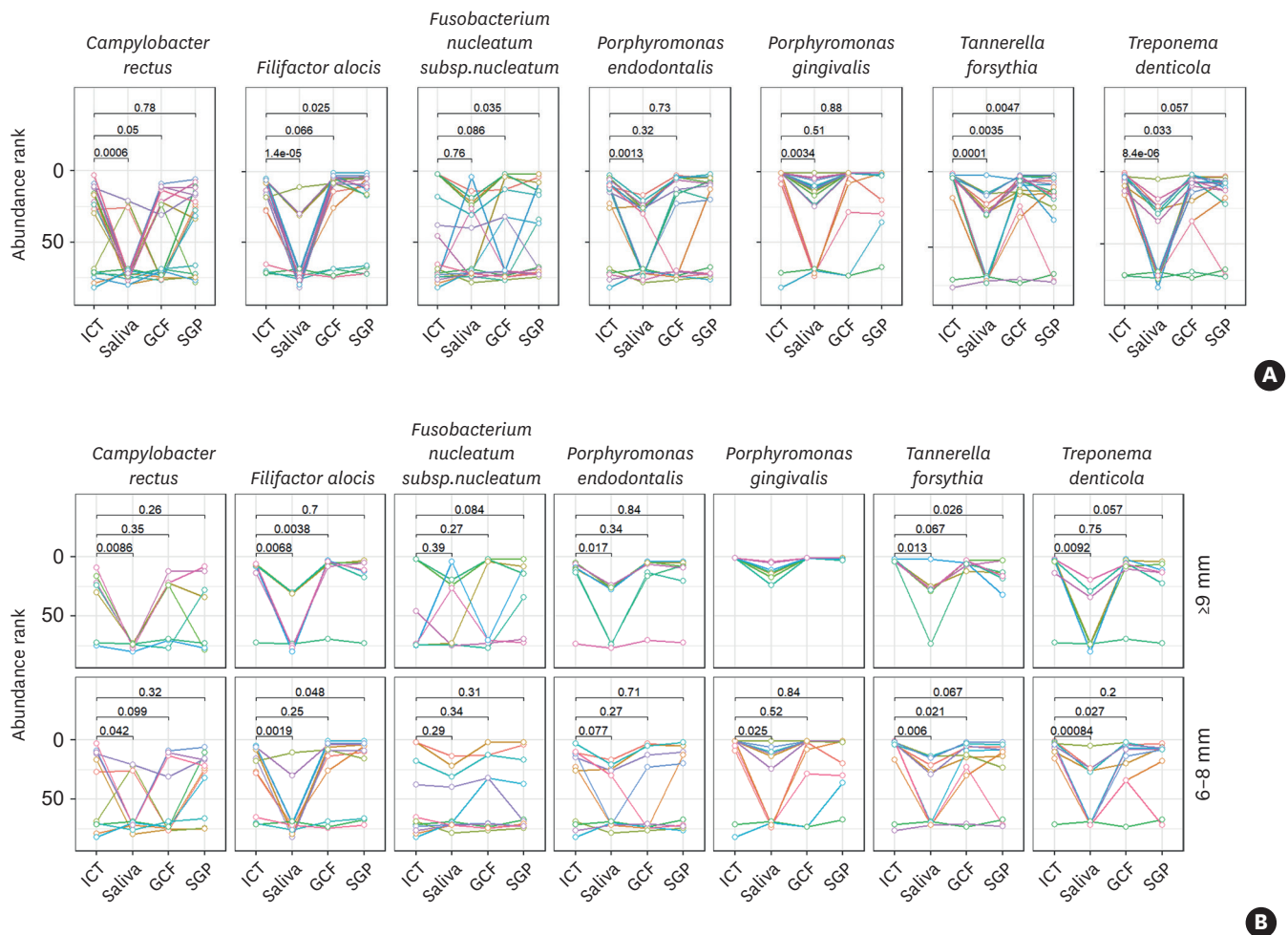


Figure 5. Abundance ranks of peri-implantitis pathogenic species among ICT, saliva, SGP, and GCF. (A) Abundance ranks of peri-implant pathogenic species (*Campylobacter rectus*, *Filifactor alocis*, *Fusobacterium nucleatum*, *Porphyromonas endodontalis*, *Porphyromonas gingivalis*, *Tannerella forsythia*, and *Treponema denticola*) across sample types. *P. gingivalis*, *T. forsythia*, *T. denticola*, *C. rectus*, *F. alocis*, and *P. endodontalis* exhibited significantly higher ranks in ICT than in saliva. (B) Subgroup analyses of the deep- and moderate-PD groups. In the deep-PD group, *P. gingivalis* had a high abundance rank across all paired samples. ICT: inflammatory connective tissue, GCF: gingival crevicular fluid, SGP: subgingival plaque, PD: probing depth.

The microbial differences between saliva and the other samples in this study were greater in patients with deep PD (PD ≥ 9 mm). Previous investigations of SGP in periodontitis also identified significant differences between deep and shallow sites, primarily due to higher abundances of pathogenic species such as *P. gingivalis*, *T. denticola*, *T. forsythia*, and *F. alocis* at deep sites (PD ≥ 7 mm) [26]. While the threshold for deep PD in our study (≥ 9 mm) differs from that used in prior periodontitis studies (≥ 7 mm), the overall trend is consistent: deeper PD is associated with increased presence of pathogenic species. Additionally, because peri-implantitis and periodontitis differ in tissue characteristics and disease progression, direct comparisons of numerical PD cutoffs across studies should be made with caution.

The environment at the base of the periodontal pocket is anaerobic and characterized by active tissue destruction due to inflammation. This differs markedly from the overall oral environment; consequently, saliva-derived microbiome data may not accurately capture critical aspects of disease progression. Furthermore, relative to site-specific samples, saliva samples are more strongly influenced by general factors unrelated to disease that can affect

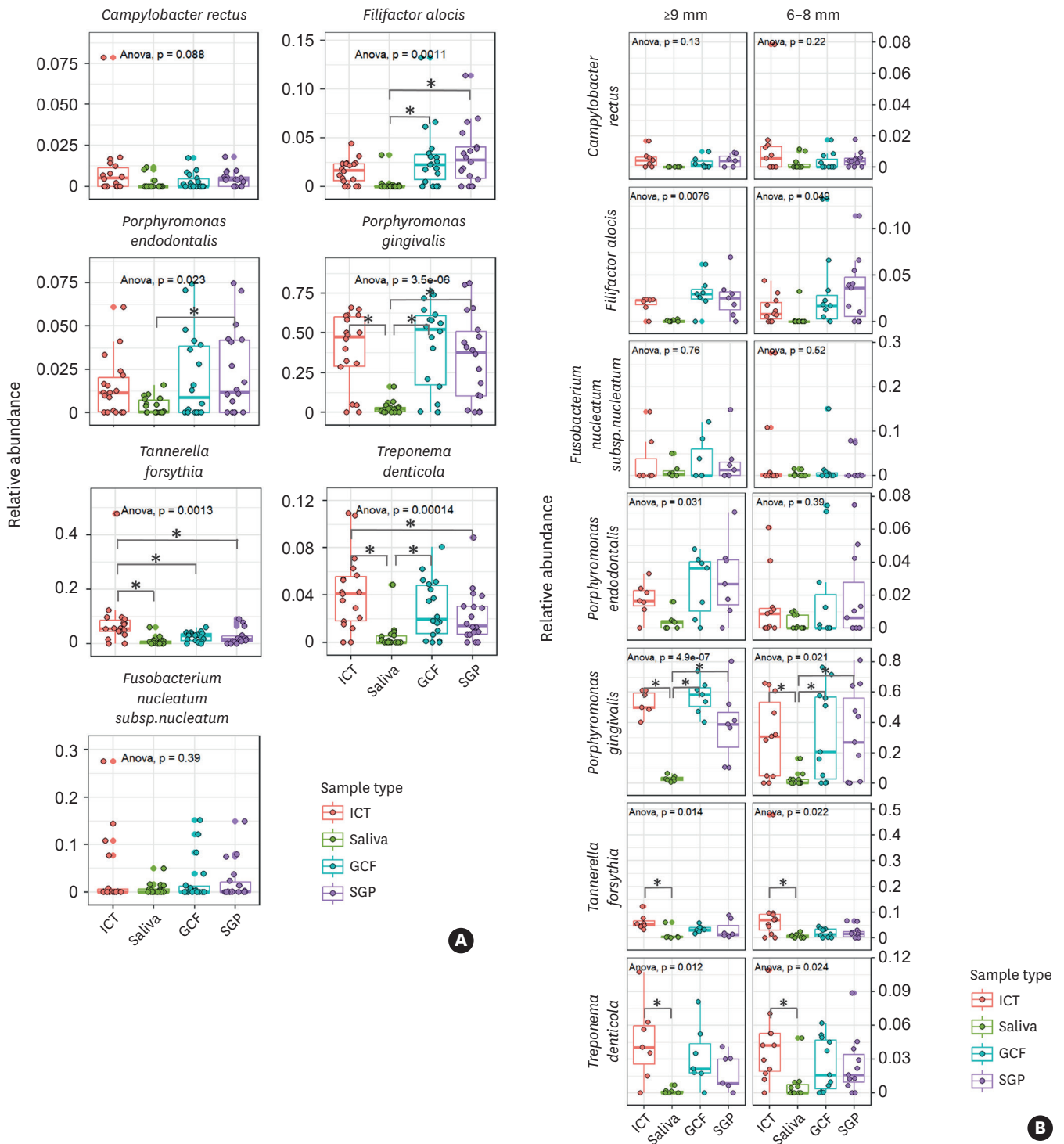


Figure 6. Relative abundances of peri-implantitis pathogenic species among ICT, saliva, SGP, and GCF. (A) The red-complex species (*P. gingivalis*, *T. forsythia* and *T. denticola*) differed significantly in relative abundance by sample type. (B) The relative abundance of *P. gingivalis* was lower in saliva, whereas those of *T. forsythia* and *T. denticola* were higher in ICT, especially in the deep-probing depth group. ICT: inflammatory connective tissue, GCF: gingival crevicular fluid, SGP: subgingival plaque.

the saliva microbiome, such as sociodemographic characteristics and antibiotic use [6,27,28]. Caution is therefore warranted when interpreting microbial analyses based on saliva samples obtained from patients with peri-implantitis.

Peri-implantitis is considered a plaque-induced inflammatory condition associated with dysbiosis of the peri-implant microbiome. This dysbiosis typically involves increased species richness in the submucosal microbiome, accompanied by significant increases in pathogenic microorganisms from the red and orange complexes [22]. These changes are evident in 16S rRNA sequencing data from GCF and SGP, where, following peri-implantitis treatment, the microbiome of the affected site shifts toward a profile with fewer red-complex bacteria and reduced diversity [14,15]. However, few studies have analyzed the microbial profile of peri-implantitis lesions using ICT. Unlike GCF and plaque samples, ICT is likely to contain bacteria capable of invading the sulcular epithelium and evading host defenses [29]. Nonetheless, in the present study, ICT displayed a microbial profile similar to those of SGP and GCF.

Host tissue is present in collected ICT samples, enabling analysis of host–microbe interactions through human complementary DNA and single-cell RNA sequencing while providing insights into the molecular mechanisms of host defense. A previous investigation of ICT from peri-implantitis sites revealed disease mechanisms via transcriptome profiling [30]. Additionally, single-cell RNA sequencing of ICT enables analysis of inflammatory modulation among cellular components involved in periodontal inflammation [9]. Therefore, ICT-based microbiome analysis offers a methodological advantage for interpreting microbiome alterations in relation to the host immune response [31]. Selecting appropriate sampling methods is essential for accurately characterizing the microbial environment at diseased peri-implant sites. Because ICT, GCF, and SGP showed similar microbial signatures, whereas saliva displayed a distinct profile, sampling strategies for peri-implant microbiome studies and diagnostics should prioritize tissue- or sulcus-based sources. Future studies integrating host transcriptomics or proteomics with microbial profiling of ICT may further elucidate the mechanisms of peri-implantitis and facilitate more targeted, host-tailored interventions.

Although host transcriptomic analyses were not performed in the present study, the ICT samples inherently contain host-derived components, offering a valuable opportunity for integrative studies of both the microbiome and the host immune response. Future analyses using these preserved ICT samples—such as single-cell RNA sequencing or bulk transcriptomic profiling—are expected to improve our understanding of host–microbe interactions involved in the pathogenesis of peri-implantitis.

The relative abundances of *T. denticola* and *T. forsythia* were significantly higher in ICT from deep-PD sites than in saliva, while that of *P. gingivalis* was significantly lower in saliva than in the other sample types. A previous study using DNA–DNA hybridization of SGP identified these 3 bacteria, associated with the severity of periodontitis, as the red complex [32]. Studies applying 16S rRNA sequencing to SGP have further confirmed that the red complex plays a pivotal role in the progression of peri-implantitis [12–14]. The red complex contributes to periodontitis by producing enzymes that destroy host tissue and by modulating the immune system, allowing these pathogens to invade tissue [11,33]. Because the ICT contains pathogenic species capable of invading tissue from the oral cavity, the higher relative abundance of the red complex likely reflects the invasive nature of these pathogens.

This study had several limitations. First, the overall sample was small. The oral microbiome exhibits significant interindividual variability while also fluctuating over time in a single individual [6,34]. Given the extensive information provided by 16S rRNA sequencing, larger samples may be necessary for disease-related changes to be distinguished statistically from individual differences. Therefore, while this study identified differences in the microbiome between sampling sites within the same individual, the small sample size limits the generalizability of the findings and the ability to fully analyze the microbial profile of peri-implantitis. Second, despite efforts to prevent cross-contamination, potential mixing of GCF and SGP during sample collection cannot be completely ruled out, possibly influencing the microbial profiles. Lastly, missing records meant that the implant type was not standardized. Titanium particles generated by corrosion in an inflammatory environment can alter the microbiome, and such factors may vary depending on the type of implant used [35]. This variability in implant materials and design could introduce additional confounding factors that were not controlled for in this study.

In conclusion, this study demonstrated that ICT, GCF, and SGP from peri-implantitis sites shared similar microbial profiles, whereas saliva exhibited a distinct microbial community structure, particularly at sites with deeper PD (PD ≥ 9 mm). Moreover, ICT, GCF, and SGP showed higher abundances of peri-implantitis-associated pathogenic species compared with saliva. Although saliva sampling is convenient and non-invasive, it may fail to capture site-specific pathogenic shifts that are more accurately reflected in localized samples such as ICT, GCF, or SGP. These findings underscore the need for carefully selected sampling strategies in both clinical and research settings to ensure precise characterization of microbial dysbiosis in peri-implantitis. ICT sampling, in particular, may provide valuable insights into the host-microbe interface, facilitating the exploration of disease mechanisms through integrated microbial and host-response analyses. Future studies involving larger cohorts and standardized implant systems are warranted to validate and expand upon the present findings.

SUPPLEMENTARY MATERIALS

Supplementary Table 1

Shannon diversity index across sample types

Supplementary Figure 1

Rank-abundance correlations of microbial species between ICT and other sample types.

REFERENCES

1. Berglundh T, Armitage G, Araujo MG, Avila-Ortiz G, Blanco J, Camargo PM, et al. Peri-implant diseases and conditions: consensus report of workgroup 4 of the 2017 World Workshop on the Classification of Periodontal and Peri-Implant Diseases and Conditions. *J Periodontol* 2018;89 Suppl 1:S313-8. [PUBMED](#) | [CROSSREF](#)
2. Hong I, Koo KT, Oh SY, Park HW, Sanz-Martín I, Cha JK. Comprehensive treatment protocol for peri-implantitis: an up-to date narrative review of the literature. *J Periodontal Implant Sci* 2024;54:295-308. [PUBMED](#) | [CROSSREF](#)
3. Mombelli A, van Oosten MA, Schurch E Jr, Lang NP. The microbiota associated with successful or failing osseointegrated titanium implants. *Oral Microbiol Immunol* 1987;2:145-51. [PUBMED](#) | [CROSSREF](#)

4. Kumar PS, Mason MR, Brooker MR, O'Brien K. Pyrosequencing reveals unique microbial signatures associated with healthy and failing dental implants. *J Clin Periodontol* 2012;39:425-33. [PUBMED](#) | [CROSSREF](#)
5. Sanz-Martin I, Doolittle-Hall J, Teles RP, Patel M, Belibasakis GN, Hämmerle CHF, et al. Exploring the microbiome of healthy and diseased peri-implant sites using Illumina sequencing. *J Clin Periodontol* 2017;44:1274-84. [PUBMED](#) | [CROSSREF](#)
6. Mangal U, Noh K, Lee S, Cha JK, Song JS, Cha JY, et al. Multistability and hysteresis in states of oral microbiota: Is it impacting the dental clinical cohort studies? *J Periodontol Res* 2023;58:381-91. [PUBMED](#) | [CROSSREF](#)
7. Kim YT, Jeong J, Mun S, Yun K, Han K, Jeong SN. Comparison of the oral microbial composition between healthy individuals and periodontitis patients in different oral sampling sites using 16S metagenome profiling. *J Periodontal Implant Sci* 2022;52:394-410. [PUBMED](#) | [CROSSREF](#)
8. Song L, Lu H, Jiang J, Xu A, Huang Y, Huang JP, et al. Metabolic profiling of peri-implant crevicular fluid in peri-implantitis. *Clin Oral Implants Res* 2024;35:719-28. [PUBMED](#) | [CROSSREF](#)
9. Easter QT, Fernandes Matuck B, Beldorati Stark G, Worth CL, Predeus AV, Fremin B, et al. Single-cell and spatially resolved interactomics of tooth-associated keratinocytes in periodontitis. *Nat Commun* 2024;15:5016. [PUBMED](#) | [CROSSREF](#)
10. Dionigi C, Larsson L, Carcuac O, Berglundh T. Cellular expression of DNA damage/repair and reactive oxygen/nitrogen species in human periodontitis and peri-implantitis lesions. *J Clin Periodontol* 2020;47:1466-75. [PUBMED](#) | [CROSSREF](#)
11. Rajakaruna GA, Negi M, Uchida K, Sekine M, Furukawa A, Ito T, et al. Localization and density of *Porphyromonas gingivalis* and *Tannerella forsythia* in gingival and subgingival granulation tissues affected by chronic or aggressive periodontitis. *Sci Rep* 2018;8:9507. [PUBMED](#) | [CROSSREF](#)
12. Yu PS, Tu CC, Wara-Aswapati N, Wang CY, Tu YK, Hou HH, et al. Microbiome of periodontitis and peri-implantitis before and after therapy: long-read 16S rRNA gene amplicon sequencing. *J Periodontol Res* 2024;59:657-68. [PUBMED](#) | [CROSSREF](#)
13. Jia P, Guo X, Ye J, Lu H, Yang J, Hou J. Microbiome of diseased and healthy implants-a comprehensive microbial data analysis. *Front Cell Infect Microbiol* 2024;14:1445751. [PUBMED](#) | [CROSSREF](#)
14. Sun F, Wei Y, Li S, Nie Y, Wang C, Hu W. Shift in the submucosal microbiome of diseased peri-implant sites after non-surgical mechanical debridement treatment. *Front Cell Infect Microbiol* 2023;12:1091938. [PUBMED](#) | [CROSSREF](#)
15. Philip J, Buijs MJ, Pappalardo VY, Crielaard W, Brandt BW, Zaura E. The microbiome of dental and peri-implant subgingival plaque during peri-implant mucositis therapy: a randomized clinical trial. *J Clin Periodontol* 2022;49:28-38. [PUBMED](#) | [CROSSREF](#)
16. Cho YD, Cho ES, Song JS, Kim YY, Hwang I, Kim SY. Standard operating procedures for the collection, processing, and storage of oral biospecimens at the Korea Oral Biobank Network. *J Periodontal Implant Sci* 2023;53:336-46. [PUBMED](#) | [CROSSREF](#)
17. Lee CH, Chen YW, Tu YK, Wu YC, Chang PC. The potential of salivary biomarkers for predicting the sensitivity and monitoring the response to nonsurgical periodontal therapy: a preliminary assessment. *J Periodontol Res* 2018;53:545-54. [PUBMED](#) | [CROSSREF](#)
18. Gerber J, Wenaweser D, Heitz-Mayfield L, Lang NP, Persson GR. Comparison of bacterial plaque samples from titanium implant and tooth surfaces by different methods. *Clin Oral Implants Res* 2006;17:1-7. [PUBMED](#) | [CROSSREF](#)
19. Callahan BJ, McMurdie PJ, Rosen MJ, Han AW, Johnson AJ, Holmes SP. DADA2: high-resolution sample inference from Illumina amplicon data. *Nat Methods* 2016;13:581-3. [PUBMED](#) | [CROSSREF](#)
20. McMurdie PJ, Holmes S. phyloseq: an R package for reproducible interactive analysis and graphics of microbiome census data. *PLoS One* 2013;8:e61217. [PUBMED](#) | [CROSSREF](#)
21. Gu Z. Complex heatmap visualization. *Imeta* 2022;1:e43. [PUBMED](#) | [CROSSREF](#)
22. Belibasakis GN, Manoil D. Microbial community-driven etiopathogenesis of peri-implantitis. *J Dent Res* 2021;100:21-8. [PUBMED](#) | [CROSSREF](#)
23. Farina R, Filippi M, Brazzioli J, Tomasi C, Trombelli L. Bleeding on probing around dental implants: a retrospective study of associated factors. *J Clin Periodontol* 2017;44:115-22. [PUBMED](#) | [CROSSREF](#)
24. Zaura E, Pappalardo VY, Buijs MJ, Volgenant CMC, Brandt BW. Optimizing the quality of clinical studies on oral microbiome: a practical guide for planning, performing, and reporting. *Periodontol* 2000 2021;85:210-36. [PUBMED](#) | [CROSSREF](#)
25. Zhang M, Zhao Y, Umar A, Zhang H, Yang L, Huang J, et al. Comparative analysis of microbial composition and functional characteristics in dental plaque and saliva of oral cancer patients. *BMC Oral Health* 2024;24:411. [PUBMED](#) | [CROSSREF](#)

26. Pérez-Chaparro PJ, McCulloch JA, Mamizuka EM, Moraes ADCL, Faveri M, Figueiredo LC, et al. Do different probing depths exhibit striking differences in microbial profiles? *J Clin Periodontol* 2018;45:26-37. [PUBMED](#) | [CROSSREF](#)
27. Renson A, Jones HE, Beghini F, Segata N, Zolnik CP, Usyk M, et al. Sociodemographic variation in the oral microbiome. *Ann Epidemiol* 2019;35:73-80.e2. [PUBMED](#) | [CROSSREF](#)
28. Karadayı B, Karaismailoğlu B, Karadayı S, Arslan A, Gözen ED, Özbek T. The uselessness of using salivary microbiota in forensic identification purposes of a person with recent antibiotic use. *Leg Med (Tokyo)* 2024;69:102338. [PUBMED](#) | [CROSSREF](#)
29. Park JY, Han D, Park Y, Cho ES, In Yook J, Lee JS. Intracellular infection of *Cutibacterium acnes* in macrophages of extensive peri-implantitis lesions: a clinical case series. *Clin Implant Dent Relat Res* 2024;26:1126-34. [PUBMED](#) | [CROSSREF](#)
30. Becker ST, Beck-Broichsitter BE, Graetz C, Dörfer CE, Wiltfang J, Häsler R. Peri-implantitis versus periodontitis: functional differences indicated by transcriptome profiling. *Clin Implant Dent Relat Res* 2014;16:401-11. [PUBMED](#) | [CROSSREF](#)
31. Ganesan SM, Dabdoub SM, Nagaraja HN, Mariotti AJ, Ludden CW, Kumar PS. Biome-microbiome interactions in peri-implantitis: a pilot investigation. *J Periodontol* 2022;93:814-23. [PUBMED](#) | [CROSSREF](#)
32. Socransky SS, Haffajee AD, Cugini MA, Smith C, Kent RL Jr. Microbial complexes in subgingival plaque. *J Clin Periodontol* 1998;25:134-44. [PUBMED](#) | [CROSSREF](#)
33. Schäffer C, Andrukhov O. The intriguing strategies of *Tannerella forsythia*'s host interaction. *Front Oral Health* 2024;5:1434217. [PUBMED](#) | [CROSSREF](#)
34. Arredondo A, Álvarez G, Isabal S, Teughels W, Laleman I, Contreras MJ, et al. Comparative 16S rRNA gene sequencing study of subgingival microbiota of healthy subjects and patients with periodontitis from four different countries. *J Clin Periodontol* 2023;50:1176-87. [PUBMED](#) | [CROSSREF](#)
35. Kotsakis GA, Olmedo DG. Peri-implantitis is not periodontitis: scientific discoveries shed light on microbiome-biomaterial interactions that may determine disease phenotype. *Periodontol* 2000 2021;86:231-40. [PUBMED](#) | [CROSSREF](#)